The Journal of Experimental Biology 203, 2933–2943 (2000)
Printed in Great Britain © The Company of Biologists Limited 2000
JEB2910



# THE HIND WING OF THE DESERT LOCUST (*SCHISTOCERCA GREGARIA* FORSKÅL)

## II. MECHANICAL PROPERTIES AND FUNCTIONING OF THE MEMBRANE

C. W. SMITH[1,2], R. HERBERT[1], R. J. WOOTTON[1,*] AND K. E. EVANS[2]

[1]*School of Biological Sciences, University of Exeter, Hatherly Laboratories, Prince of Wales Road, Exeter EX4 4PS, UK* and [2]*School of Engineering and Computer Science, University of Exeter, Exeter EX4 4QF, UK*

*Author for correspondence (e-mail: r.j.wootton@exeter.ac.uk)

*Accepted 29 June; published on WWW 7 September 2000*

**Summary**

**As part of an investigation of the functional mechanics of the hind wing of the desert locust *Schistocerca gregaria*, the Young's modulus of the membrane was measured using a newly developed universal materials test machine capable of testing very small specimens of cuticle, down to 1 mm gauge length. Strain was measured optically. Specimens were cut from various locations around the wing and tested under controlled temperature and humidity. The modulus of the membrane was typically between 1 and 5 GPa, but both this and the membrane thickness varied around the wing, with the remigium and the anal fan showing markedly different properties. The membrane was tested for chitin using two methods: a gas pyrolysis/mass spectrometry assay, and a gold-labelled immunoassay specific to chitin. None was detected, and the membrane may consist of epicuticle alone. The wings were examined for evidence of crystalline material using standard polarising microscopy and an advanced technique that distinguishes between three components of the polarised image. Birefringence was detected in the membrane of the anterior part of the wing, but vanished when the membrane was separated from the surrounding veins, suggesting that it was due to pre-stress rather than to ultrastructure. The implications are discussed.**

Key words: locust, *Schistocerca gregaria*, wing, material properties, chitin.

### Introduction

The wings of insects contain no muscles. In flight, their cyclically varying three-dimensional shape is determined partly by forces exerted by controlling muscles and skeletal components at the extreme base and partly by the detailed structure of the wings themselves responding aeroelastically and usefully to the inertial and aerodynamic forces. This level of automatic shape control in propulsive appendages is probably unique in the animal kingdom (Wootton, 1999) and appears to be the principal reason for the huge morphological variety of insect wings, far greater than that in flying vertebrates.

As with all complex structures, their mechanical responses to loads are due partly to gross structure (relief, the flexibility and torsional compliance of individual components, how these are linked together in three dimensions) and partly to the properties of the materials from which these components are constructed. Both gross structure and material properties need to be taken into account in any rigorous engineering analysis.

This, the second of three papers on the mechanics of the hind wing of *Schistocerca gregaria* Forskål, is concerned with the material properties of the wing membrane cuticle. In the first paper (Wootton et al., 2000), it was shown that the membrane is not simply a barrier to the passage of air through the wing but, in some areas at least, has a structural role as a stressed skin, stiffening the framework of veins. Elsewhere, the development of deep tension creases in the membrane indicate considerable deformation. This is particularly true in the anojugal fan (the 'vannus' of Snodgrass, 1935) during the semi-automatic development of camber as a result of wing promotion during the downstroke: the so-called 'umbrella effect' (Wootton, 1995). For more details of the remigium and anal fan, see Wootton et al. (2000). These apparent differences suggest that there may be local variation in the mechanical properties and, hence, in the structure of the membrane within the wing, with profound implications for its functioning in flight.

The general organisation of insect cuticle is well known (Richards, 1951; Neville, 1975). Two main layers are usually distinguished: the epicuticle, seldom more than 1.5 μm thick, and the procuticle, whose thickness can reach several millimetres. Each is further subdivided. The mechanically significant sublayers of the epicuticle are the 'outer epicuticle', approximately 18 nm thick, and probably consisting of highly polymerised hydrocarbons, and the 'inner epicuticle', 0.5–2.0 μm thick, which appears to be mainly protein, with lipid and polyphenol inclusions (Neville, 1975; Filshie, 1982).

So far as is known, the epicuticle contains no chitin. The procuticle, generally by far the thicker layer, consists of chitin microfibrils, normally approximately 20 nm in diameter, in a matrix of proteins and acting as a fibrous composite (Vincent, 1980; Neville, 1993). Over much of the body surface it makes up an outer 'exocuticle' in which the proteins are highly cross-linked and an inner, more compliant 'endocuticle', generally laid down after ecdysis, in which the proteins are scarcely cross-linked. Between these more rigid skeletal areas – the 'sclerites' – the procuticle is a pliant 'arthrodial membrane' resembling, but not identical with, the endocuticle.

Most insect cuticle fits this basic plan, but with many variations. The most obvious is the thickness of the cuticle as a whole and of the individual layers. Other variables include the proteins present (approximately 100 have been recognised; Andersen et al., 1995), the degree and nature of the cross-linking (Andersen et al., 1996; Vincent and Hillerton, 1979), the ratio of protein to chitin and the alignment of the chitin microfibrils (Neville, 1975). All these can be expected to influence the mechanical properties of the composite procuticle (Vincent, 1980; Neville, 1993), often very locally, because the details of cuticle secretion may vary from epidermal cell to epidermal cell.

The considerable problems of accurately measuring the properties of samples that are necessarily small have limited the number of attempts to characterise cuticle materials mechanically (Jensen and Weis-Fogh, 1962; Vincent, 1975; Reynolds, 1975; Hepburn and Chandler, 1976; Ker, 1977; Vincent and Hillerton, 1979; for reviews, see Vincent, 1980, 1990). Reliable values for Young's modulus range from 11 GPa for the tibial apodeme of the locust jumping leg, in which the chitin microfibrils are very highly aligned (Ker, 1977), to 0.25 GPa for wet tanned *Calliphora vomitoria* puparium (Vincent and Hillerton, 1979) and 2.2 MPa for the ligaments of the dragonfly *Aeshna grandis*, which consist only of the elastomeric protein resilin (Weis-Fogh, 1961; Vincent, 1980).

The picture emerging from these studies is of a material, or family of materials, with a remarkable range of properties suited to its many roles. These include energy-storing springs, compliant connective tissue, stiff tensile tendons, hard, abrasive and abrasion-resistant surfaces and many tools and other structures with special mechanical requirements.

The cuticle of wings has hardly been studied. The only published value for the Young's modulus of wing cuticle appears to 6.1 GPa for the calliphorid fly *Phormia regina* (C. J. C. Rees, quoted in Wainwright et al., 1976), without information as to how it was obtained. The only ultrastructural studies are those of Banerjee (1988a,b) on the wings of various Orthoptera. These included *Schistocerca gregaria*, but investigations on this species appear to have been limited to the fore wing, which is partly adapted for a protective role, with an extensively thickened membrane, and has no anal fan. The hindwing membrane is of interest not only because of its role in the functioning of the wing but also as an example of ultra-thin insect cuticle. Other examples include the walls of the air-sacs of the respiratory system (Wasserthal, 1996) and the larval cuticle of chironomid fly larvae (Credland, 1978). It is difficult to reconcile these membranes with the standard model of cuticle described above; their thickness is often comparable with that of the epicuticle alone.

We have therefore developed a sensitive mechanical testing rig capable of accurate measurements on tiny specimens and have used it to map the tensile stiffness of membrane around the locust hind wing. To examine whether the membrane consists of epicuticle only, we have, in parallel with these tests, assayed for chitin using a combined gas pyrolysis/mass spectrometry technique (Stankiewicz et al., 1996) and a gold-labelled wheatgerm immunoassay (Lemburg, 1998).

Polarising microscopy has previously detected birefringence in the membrane of the anterior part of the wing (R. J. Wootton, unpublished data). Further investigation has been necessary to determine whether this is the rule and to determine its nature, cause and significance, if any, in the functioning of the wing. Besides standard equipment, we have had access to a novel method developed in the Department of Physics, University of Oxford, which has already proved useful in examining insect wings (Glazer et al., 1996).

## Materials and methods

### *Preparation*

*Schistocerca gregaria* Forskål were bought as late fifth-instar nymphs and kept in a controlled-temperature room at 25 °C until the final moult. They were then removed to a cage with a light bulb for warmth in a laboratory. Food and water were provided daily and were available *ad libitum*. One individual at a time was selected for testing and marked with a white paint spot on the tergum for easy retrieval. Specimens were taken from the same individual until its natural death. Three insects were tested. One wing of the locust was spread out under a stereo microscope, a small number of cells were cut out, and the locust was returned to the cage. A thin, parallel-sided strip (approximately 0.1–0.2 mm) was cut from the cells with its length either in the basal–distal axis of the whole wing or normal to it. The strip and remaining cells were placed into a humidity cabinet at 80 % relative humidity to minimise water loss.

A rough rectangle of aluminium foil (usually 4 mm×3 mm and approximately 0.01 mm thick) was cut under a stereo microscope, the exact size depending on the size of the specimen. A smaller rectangular section inside was cut out to leave a frame, and sections from both ends were cut away leaving two 'tabs' that could be folded over flush with the frame (Fig. 1). A thin strip specimen cut from the wing cells was removed from the humidity cabinet and placed into the aluminium rectangle, and the tabs on the aluminium frame were folded over to cover the ends of the specimen. A small drop of cyanoacrylate adhesive was placed at the edge of the aluminium tabs so that capillary attraction would draw the adhesive underneath the folded tab and cement the specimen to the aluminium. In this way, strong frames were placed

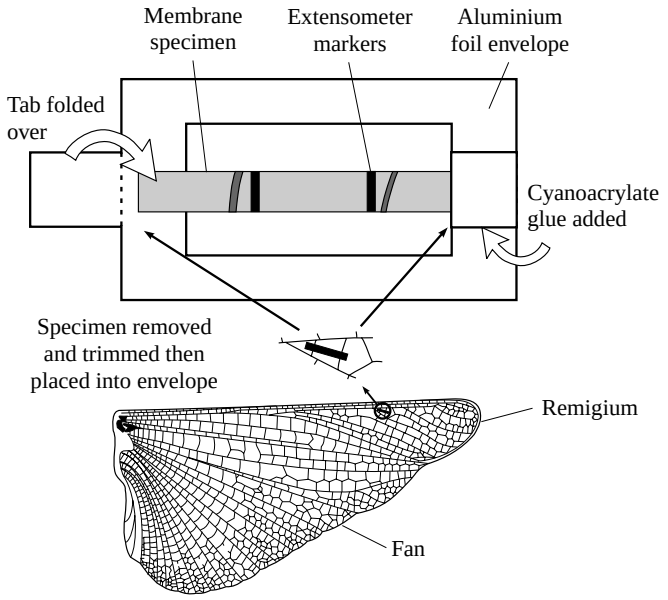


Fig. 1. Diagram of the frames used to mount the specimens into the testing machine.

around delicate specimens, protecting them during mounting into the test machine.

A small strip of carbon copy paper was cut with a razor blade, its rear surface was sprayed with poster-mounting glue and it was placed onto waxed paper. Two very small strips of the carbon copy paper were then cut with a razor blade (typically 0.3 mm long×30 μm wide) and transferred onto the surface of the specimen in its frame whilst under the microscope. These black strips acted as markers for the strain-measuring system. Specimens were regularly returned to the humidity cabinet during the dissection, mounting and marking processes so that they were never outside a humid environment for more than 10 min at a time. Fibre optic illumination was used at all times. It was hoped that these procedures would prevent water loss from the specimens.

The humidity cabinet was a large clear plastic, airtight cabinet. Inside the cabinet was a pump delivering air to several 'air stones' (normally used for aerating fish tanks). The air stones were just submerged in water so that the air blew up a fine spray of water. This had the effect of rapidly increasing the relative humidity of the air inside the cabinet. Specimens were tested in another smaller chamber which itself sat inside a temperature-controlled incubation cabinet. A small fan circulated humid air between the humidity chamber and the small test chamber *via* two lengths of flexible tubing. A humidity sensor was mounted inside the small test chamber. The desired relative humidity could be entered into a control box that read the humidity sensor and switched the pump in the humidity chamber on or off as needed. In this manner, the relative humidity inside the humidity cabinet and the small test chamber could be kept constant (±1 %) between ambient and 95 % relative humidity. Separate humidity sensors were used to check the system and found it to be accurate and steady.

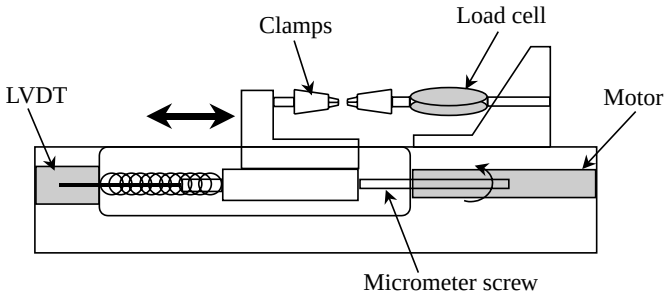


Fig. 2. Schematic diagram of the important elements of the universal testing machine. LVDT, linear variable displacement transducer. See text for further details.

### *Mechanical testing*

The test machine was similar in concept to a standard materials test machine but mounted horizontally (Fig. 2). The specimen was held by two clamps, one attached to a load cell, the other to a movable cross head. The cross head was mounted on two 'frictionless' bearings and connected *via* a diamond chip and steel ball bearing to a rod with a micrometer thread housed in the machine's frame. A brushless direct current motor in line with the load cell and cross head turned the micrometer threaded rod, which moved the cross head towards or away from the load cell. An in-line linear variable displacement transducer (or differential transformer) (LVDT) measured the displacement of the cross head; the motor's movement could also be measured by counting its revolutions. The load cell had an accuracy of nearly ±150 μN with a maximum capacity of 10 N, the LVDT an accuracy of ±60 nm and a total stroke length of 10 mm and the motor a minimum displacement movement of 1 μm and a total stroke length of 10 mm. The test machine was controlled by a PC with specially written software.

The clamps were designed and built in-house. They were of the wedge type but consisted of two semicircular-section stainless-steel rods with a taper, contained in a tight-fitting tapered stainless-steel tube. A spring mounted at the rear of the two wedges forced them forward inside the tapered tube, which pushed them together. A pin was placed in one of the wedges so that an operator could manually draw the wedges backwards, and thus apart, to mount specimens inside. The surfaces of the wedges were sand-blasted to improve friction with the specimen. The clamps were enclosed by the small test chamber fed with humid air from the humidity chamber. The small test chamber had two sections, the uppermost of which could be removed for mounting specimens. Once replaced, the test chamber was nearly air-tight but allowed the clamp attached to the load cell to move freely.

During mounting, the clamps were moved apart and the specimen, still in its aluminium frame, was placed in the clamp attached to the cross head. A second stereo microscope placed overhead allowed the operator to check the alignment of the specimen down the centre axis of the machine at all stages. Once in alignment, the clamps were brought together and the specimen was placed in the other clamp. The two long sides of the aluminium frame around the specimen between the

clamps were cut, allowing the specimen to be deformed. The upper section of the test chamber was replaced, and the specimen was extended until just taut.

*Video extensometer*

The overhead microscope was also used by the optical strain-measuring system; a Messphysik (GmBH) 'videoextensometer'. One light path of the microscope was diverted to a CCD camera that fed a real-time PAL signal to the videoextensometer software on a second PC. The software differentiated the intensity of the PAL signal along several rows of pixels down the centre of the specimen, the location of which was set by the operator. A white background was placed behind the semi-translucent specimens so that the black carbon copy paper strips contrasted strongly. The software could then pick out the sharp peak as the intensity signal changed rapidly from white to black going down the centre rows of pixels. It could measure the number of pixels between peaks and, if calibrated, the distance, although this was not necessary when measuring strain because strain is dimensionless. The resolution of the system was enhanced to sub-pixel distances by averaging data from multiple rows of pixels. The actual resolution of the system *in situ* was below 1 μm. The two markers could be placed on the specimen at any location, and strain was only measured between the markers. Thus, it was possible to have a relatively long specimen but to measure strain and other properties along a shorter portion. If the cross section of the specimen was constant between the markers, this system allowed the operator to isolate sections optically while they remained physically connected to their surrounding material.

The desired displacement, velocity, number of cycles and other information were entered into the software controlling the test machine, and the test was initiated. Data from the load cell, LVDT and motor were stored by the test machine software, and the videoextensometer software stored the data concerning the distance between the two markers. The specimens were placed in tension and then allowed to relax, initially by 0.01 mm, at a rate of 0.001 mm $s^{-1}$ for three or four cycles. The displacement was then increased to 0.02 mm, and the rate to 0.002 mm $s^{-1}$ for a further three or four cycles, then to 0.03 mm at 0.003 mm $s^{-1}$ for a further three or four cycles. This was continued until the specimen broke or reached 0.04 mm deformation. In all tests, the extension and relaxation phases lasted 10 s. Specimens varied in gauge length, so these displacements did not represent a precisely constant strain or strain rate, although the peak cyclic strain ranged from 0.2 to 0.4 % and the strain rate from 0.02 to 0.04 % $s^{-1}$.

*System calibration*

The instrument was designed and part-built by ourselves, so it was necessary to check its accuracy and repeatability and to measure its compliance. We performed the following tests: (i) measuring the noise of the load cell and LVDT *in situ* with the motor still and running; (ii) measuring the drift of the load cell and LVDT with time and temperature; (iii) measuring the repeatability of individual specimens; (iv) comparing the Young's modulus of a specimen of high-density polyethylene as measured on this machine and on another standard larger test machine; and (v) measuring the Young's modulus of a single Kevlar fibre (DuPont) and comparing it with the manufacturer's value. We also measured the compliance of the machine and grips themselves, i.e. the deflection of the machine plus grips caused by a unit load. This was performed by measuring the compliance of a successively shortened aluminium foil specimen. The compliance was then extrapolated back to zero specimen length.

*Test specimens*

Several sets of tests were performed, although it was possible to combine some of these tests. Briefly, four groups of tensile tests were made: (i) tests on specimens from various locations around the hind wing; (ii) tests on pairs of specimens from similar locations on the left and right wings of a particular individual; (iii) tests on two pairs of specimens from similar locations on the left and right wings, but taken in orthogonal directions; and (iv) tests on one specimen at high relative humidity (75 %) and five more times at decreasing relative humidity.

*Data analysis*

Data from both the videoextensometer and test machine software were imported to a spreadsheet package. It was then possible to match the two sets of data by identifying the start of the first displacement cycle, even though the data sets were neither synchronised nor taken at the same rate. It was observed that the behaviour of the specimens settled to a more-or-less constant pattern after a few displacement cycles, so data for analysis were taken from the third or fourth cycle of the largest displacement series. The distance data from the videoextensometer software were always linear with time because they were governed by the displacement of the motor. They could be fitted to the accompanying time data by a linear function using a least-squares method. This function was then used with the time data in the test machine software to calculate the displacement of the specimen at time intervals synchronous with the load cell, LVDT and motor position data as captured by the test machine software.

*Definitions*

The calculated distance data from the videoextensometer software were used to calculate engineering strain $e$ as:

$$e = \Delta l / l_0 , \quad (1)$$

where $\Delta l$ is the change in distance between the two markers and $l_0$ is the original distance between the two markers. The load data from the test machine software were used to calculate the stress $\sigma$ as:

$$\sigma = f/A , \quad (2)$$

where $f$ is the force on the specimen and $A$ is its cross-sectional area. The cross-sectional area was calculated as the product of the width (measured using callipers) and the thickness

(measured in a scanning electron microscope) of the specimen. The two sets of data were plotted as stress *versus* strain, the slope of which is the Young's modulus *E*. *E* was calculated using a least-squares fit to a straight line over the whole of the rising portion of the third or fourth cycle of the stress *versus* strain plot.

### *Birefringence*

The refractive index of a specimen may vary with its orientation relative to the plane of vibration of a polarised light source. In a biological material, this usually indicates inherent preferential alignment of linear molecules or supramolecular elements, 'form birefringence', or alignment/extension of molecules under tension, 'strain birefringence'.

An Olympus polarising microscope was used to examine pieces of membrane both in intact wings and cut free of the surrounding veins. A quarter-wavelength plate was inserted to determine the orientation of any birefringence (Neville, 1980). The same cells were photographed, both *in situ* and excised, at the same initial orientation under the microscope. If birefringence was apparent in the intact membrane, but lost during excision, it could be assumed to be due to strain, in a pre-stressed membrane; if it remained, a structural (form) basis would be expected.

For more critical examination, an automated microscope, developed in the Physics Department of Oxford University, was used (Glazer et al., 1996). In this, the polarising lens is rotated in steps through 360 °. The system separates the image into three components: the orientation of the optical indicatrix (normally referred to as the birefringence), the optical retardation and the transmittance. These components are converted by a PC into separate colour-coded images. The separation of the retardation signal from the indicatrix signal prevents misinterpretation of relief features as birefringent features and has the additional benefit of providing a three-dimensional survey of the material being examined. As long as the samples are placed on the microscope stage with the same initial orientation, the results can be directly compared, so that the technique is both qualitative and quantitative.

### *Biochemical assays*

Samples of membrane were isolated from the same wings as were used in the mechanical tests. These samples were carefully checked to make sure they contained no vein material. The samples were then sent to the NERC Organic Mass Spectrometry Facility at the School of Chemistry, University of Bristol, where they were assayed using combined pyrolysis/gas chromatography/mass spectrometry, following the method used by Stankiewicz et al. (1996). Briefly, the specimens were placed within quartz tubes in a helium atmosphere and pyrolised at 610 °C for 10 s, and the products were transferred to the chromatograph/mass spectrometer. Individual components were identified according to their mass spectra and chromatographic retention times, with reference to published data (Stankiewicz et al., 1996).

Several membrane 'cells', taken from various locations around the wing including the anal fan and the remigium, were used in the gold-labelled immunoassay. The samples were macerated, fixed in 3 % glutaraldehyde buffered with Tris and dehydrated through a graded ethanol series. They were then placed in LR White cold cure resin plus accelerator, which infiltrated the material. Once the resin had set, the samples were allowed to incubate with gold-labelled wheatgerm agglutinin diluted to 1:100 with Tris, buffered at pH 10.5, for 2–3 h at room temperature (about 20 °C) in a moist environment. They were then rinsed in Tris, rinsed again in 75 % Tris plus 25 % water, and so on until a final rinse in 100 % water. The samples were then fixed with biomount, and the silver enhancer was added until the silver agglomerates became visible under a stereo microscope. The reaction was then stopped with water. For further details, see Lemburg (1998).

## Results

### *Calibration and error estimation*

The noise levels of the load cell and LVDT *in situ* were approximately ±150 µN and ±150 nm, respectively, and the load cell was unaffected by activity of the motor. The load cell and LVDT were sensitive to changes in temperature, changing by $-0.023\ \mathrm{N\,°C^{-1}}$ and $0.00034\ \mathrm{mm\,°C^{-1}}$, respectively (over the range 31–35 °C). The repeatability of the whole system was indicated by the Young's modulus values for repeated tests on an ultra-high molecular mass polyethylene specimen (UHMWPE); the mean Young's modulus for this specimen was 0.575 GPa, which agrees with the value of 0.607 GPa

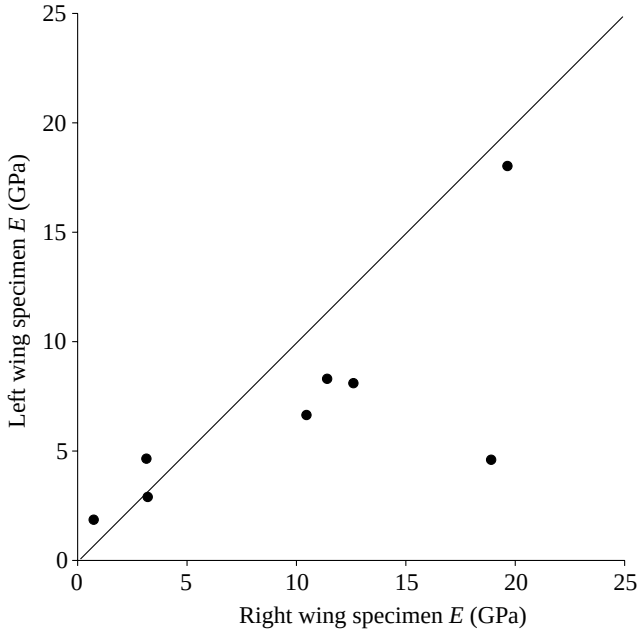


Fig. 3. Young's moduli *E* of paired specimens, i.e. from similar locations on the left and right wings of individual locusts. The line drawn is equivalence.

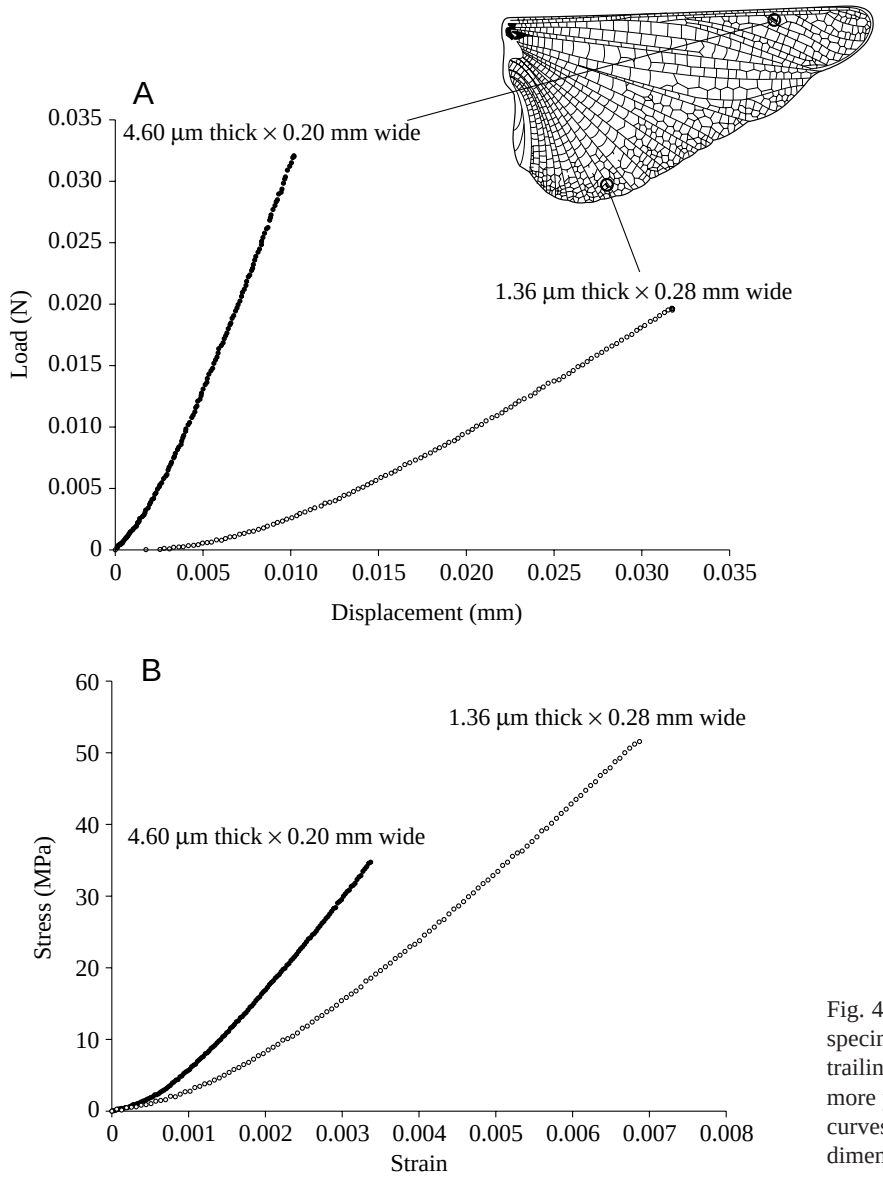


Fig. 4. (A) Typical load/displacement curves from specimens from the remigium (filled circles) and from the trailing edge of the vannus (open circles), showing the more pronounced toe region in the latter. (B) Stress/strain curves for the same two tests with the specimen dimensions noted.

found using a standard test machine for a larger sample of the same material (5 % difference). We also tested single Kevlar 49 polyaramid fibres (high-modulus yarn variety, DuPont) and found the Young's modulus to be 120 GPa, which agrees with the manufacturer's value of 120 GPa at room temperature and humidity. Finally, the compliance of the whole system, i.e. the test machine together with grips, was found to be approximately $0.0215\,\mathrm{mm\,N^{-1}}$.

In some cases, specimens from similar locations on both the left and right hind wings were successfully tested. The Young's modulus results for these left/right pairs are plotted in Fig. 3. Differences between the left and right values are due both to variability in the specimens themselves and to possible error in the testing system. We found the error of the test machine to be of the order of 5 % with the UHMWPE specimen, which was of a similar stiffness ($\mathrm{N\,mm^{-1}}$) to the wing membrane specimens.

*Mechanical tests*

Typical load/displacement curves for membrane material from the trailing edge of the vannus (anal fan region) and from the remigium are shown in Fig. 4A together with the width and thickness of the specimens. Note that the specimens were from the same individuals. Fig. 4B shows the stress/strain data for these two specimens. The Young's moduli and locations in the hind wing of all specimens tested are shown in Fig. 5. The direction in which the specimen was cut is indicated. The relationship between the Young's modulus of one particular specimen and the relative humidity of the surrounding air is shown in Fig. 6A, with the relevant stress/strain curves in Fig. 6B. The modulus of this particular specimen increased from 13.5 GPa in air at 75 % relative humidity to 16.5 GPa at 40 % relative humidity. The mean modulus from the remigium was 9.89±3.47 GPa and that in the anal fan region was 3.70±2.71 GPa (means ±

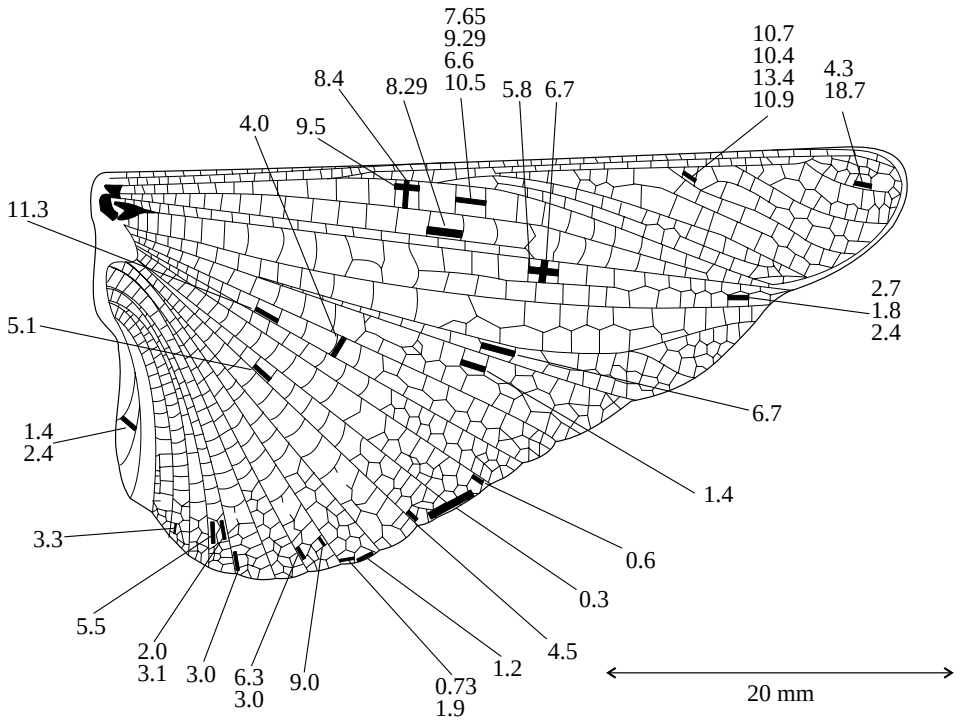


Fig. 5. Young's moduli (in GPa) from all successful tests, with the location and orientation of the specimens indicated by the filled bars. Where more than one value is given, several specimens were tested.

S.D., $N$=18 (remigium); $N$=21 (vannus)) at 75 % relative humidity.

Fig. 7 shows the thickness of the membrane at various locations around the wing. The mean membrane thickness of all the test specimens in the anal fan was 1.70±0.85 μm, whereas the mean thickness in the remigium was 3.71±1.18 μm (means ± S.D., $N$=22 (anal fan); $N$=13 (remigium)). Membrane material from the anal fan is therefore both less stiff and thinner than material from the remigium. A typical stress/strain curve of material from the trailing edge of the anal fan shows a pronounced toe region at low strain (see Fig. 4B). This membrane material is typically crinkled in appearance relative to the main wing area material.

The moduli of the two pairs of orthogonal specimens differed by –12 % and 16 % (proximal–distal specimen compared with anterior–posterior specimen), showing anisotropy no greater than that expected from experimental scatter.

### *Polarising microscopy*

Preliminary examination of hind wings with a polarising microscope revealed clear evidence of birefringence in the membrane of most individuals (Fig. 8A), but only of the cells in the anterior part of the wing (zone A of Wootton et al., 2000). This vanished when the membrane was cut free of the surrounding veins (Fig. 8B), demonstrating that the birefringence was strain-induced: the membrane was in tension

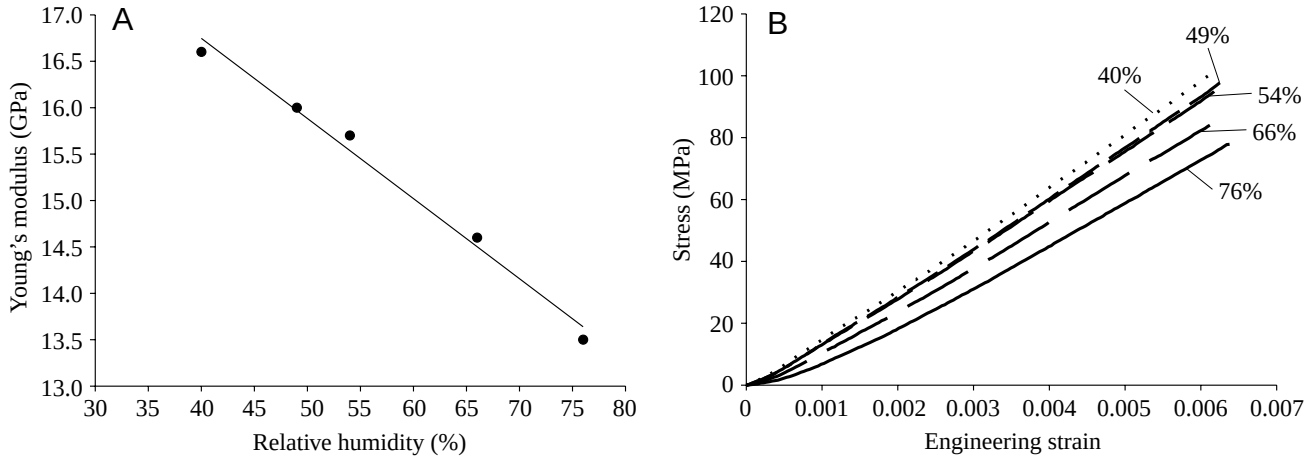


Fig. 6. (A) The relationship between Young's modulus and relative humidity for one specimen. The Young's modulus varies linearly, but only slightly, with relative humidity. (B) The stress/strain curves for the same data. The values for relative humidity are shown for each curve.

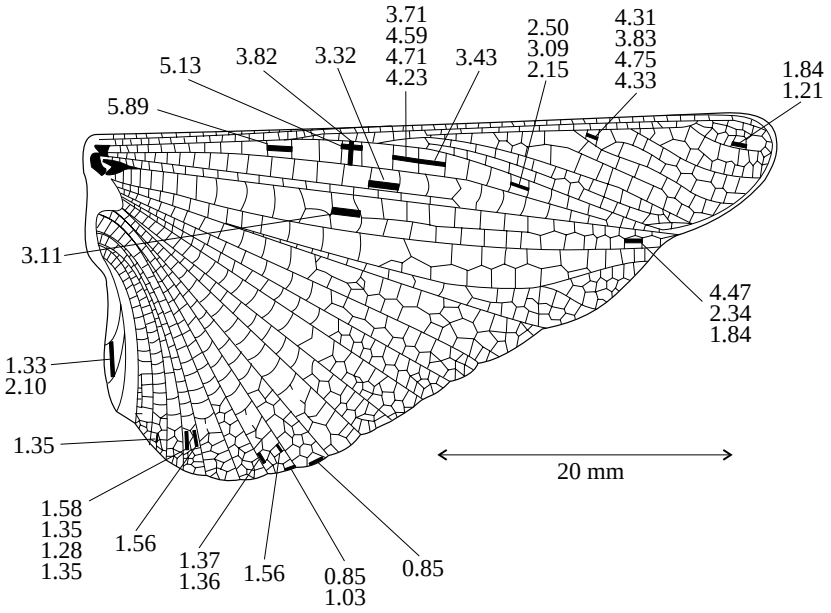


Fig. 7. Membrane thickness (in μm) at various locations around the wing. The locations and orientations of the specimens from which membrane thickness were measured are indicated by the filled bars. Where more than one value is given, the values represent repeat measurements from that site.

in the intact wing. More critical examination of wings using the automated polarising microscope developed by Glazer et al. (1996) confirmed the presence of birefringence, but indicated that the pattern of stress was more complex than was apparent under the ordinary polarising microscope (Fig. 9).

*Biochemical assay*

The mass of membrane available from single cells was insufficient for the assay techniques, so material from several locations had to be pooled. Two typical spectra from the mass spectrometry assays for the membrane material are shown in Fig. 10. The spectra show marked peaks for chitin pyrolysis products, i.e. acetic acid, acetamide, 3-acetamido-5-methylfuran and oxazoline (Stankiewicz et al., 1996), for the specimens containing venous material, which very probably contained chitin. The spectra from the specimens containing membrane only showed no trace of chitin pyrolysis products. Similarly, no chitin was detected in the membrane using the gold-label immunoassay.

We can state, therefore, that no chitin was detected in the membrane samples we tested, using the methods employed.

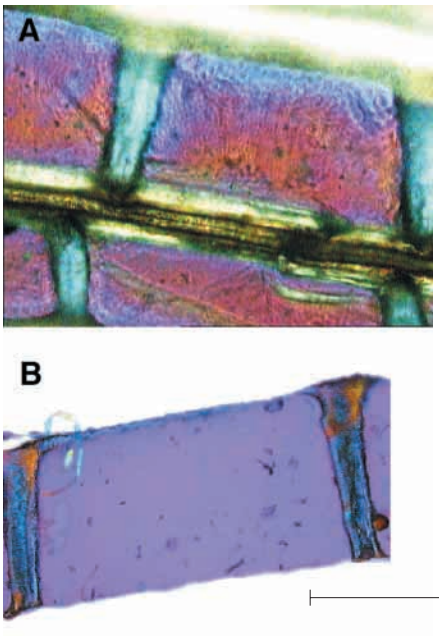


Fig. 8. Two optical micrographs of a membrane specimen *in situ* with veins attached (A) and excised (B). The birefringence disappears once the constraint of the veins is removed, indicating that there is no structural birefringence but that the membrane is in tension. Scale bar, 0.5 mm.

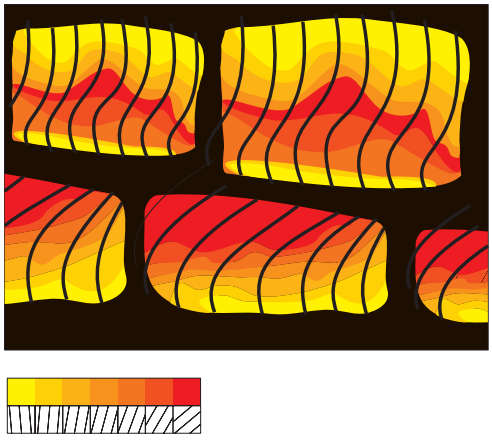

Fig. 9. Stress contours in cells in adjacent panels of the leading-edge spar, computed from images obtained using the automatic polarising microscope. The colours represent areas of different stress alignments in the membrane, as indicated by the key. The thick lines represent smoothed trajectories of the stresses themselves.

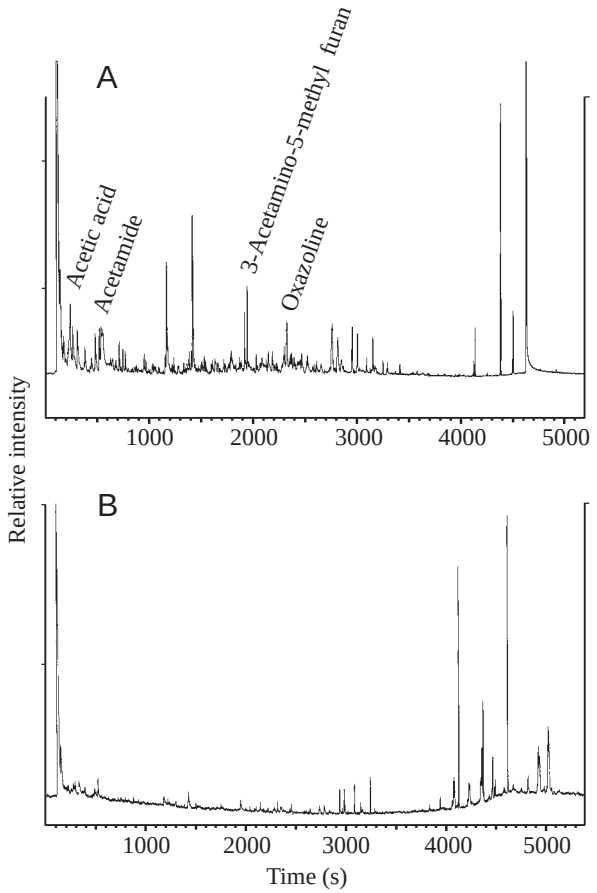


Fig. 10. Two pyrolysis mass spectra of (A) a membrane and vein sample, clearly showing chitin breakdown products (labelled peaks), and (B) a membrane-only specimen lacking chitin breakdown products. Intensities are shown relative to the highest peak.

## Discussion

The small-scale materials test machine, in combination with the videoextensometer system, was found to be reasonably accurate and stable and, in general, suitable for characterising materials such as those in insect wings. It was essential to maintain a constant temperature during tests.

Modulus values of specimens from similar locations on the left and right wings (Fig. 3) show some scatter. If we assume that the properties of these left/right pairs should be identical, this scatter would demonstrate the experimental variability of the whole testing system. With the exception of one point, the data lie reasonably near the equivalency line, indicating a reliable and accurate system.

The apparent absence of chitin from the hindwing membrane is a notable discovery and has many implications. Together with the membrane dimensions (generally 1–5 μm thick), it recalls the epicuticle layer of cuticle found elsewhere (Richards, 1951; Andersen et al., 1995), and the most probable hypothesis is that the membrane is formed by two layers of epicuticle placed back to back. Almost nothing is known of the proteins of the epicuticle, which are effectively unextractable (Andersen et al., 1995). The pyrolysis/mass spectroscopy assay of the wing membrane confirms that proteins are the principal component; the mechanical isotropy and lack of birefingence except under strain suggest that they are non-aligned or amorphous.

If the membrane does indeed consist mainly of amorphous protein, the Young's modulus values (approximately 5 GPa) are somewhat higher than expected. Some other amorphous protein polymers, e.g. resilin and abductin, have lower moduli, 1.2 MPa and 4 MPa respectively (Gosline, 1980; Alexander, 1966). Most synthetic amorphous polymers have moduli in the region of 4 GPa. Natural materials with high modulus values, such as α-keratin (4 GPa in sheep's wool), β-keratin (8–10 GPa in pigeon feathers) and lepidopteran silk (10 GPa in *Bombyx mori*) (data from various sources, quoted in Vincent, 1990), have highly aligned or crystalline molecules. Vincent (1990) has shown that the puparium (the shed cuticle of the last-instar larva, enclosing the pupa) of the fly *Calliphora vomitoria* can have modulus values in excess of 3 GPa. There, however, well-aligned chitin is present, and the cuticle tested was both tanned (covalently cross-linked) and dried in air. Indeed, Vincent and Hillerton (1979) found the drying process, and the extensive hydrogen-bonding that results, to be more important than tanning in raising the Young's modulus from its value of 73 MPa in the wet, untanned state.

The stiffness of the cuticle in the wing membrane implies a high degree of intermolecular cross-linking. It is interesting to find the Young's moduli so little affected by the relative humidity of the surrounding air, which one would expect to be reflected in the membrane's water content. This suggests that the membrane may be quite hydrophobic and may contain little water *in vivo*. Indeed, this could hardly be otherwise, given the poor connection between the membrane and any haemolymph supply. An ultra-thin membrane oscillating rapidly in air with the low humidities and high temperatures typical of the habitat of the desert locust would be very hard to keep moist. It would be wholly logical to employ a material with low sensitivity to water content. Because of the low water content, we did not take extra measures to prevent shrinkage due to dehydration in the scanning electron microscope.

Dry, high-modulus cuticle tends to be brittle. We did not attempt to find the work of fracture of our specimens, but the stress/strain curves showed little plastic strain before failure, suggesting that the membrane is not particularly tough. It seems probable that tearing is minimised by the architecture of the wing rather than by any property of the membrane.

The variation around the wing of both Young's modulus and membrane thickness (Figs 5, 7) is of profound interest in the context of the wing's functioning. The remigium as a whole is a relatively rigid plate, with moderately high relief at the base, diminishing along the span. Ablation of the membrane significantly increases the compliance of the main part of the remigium to bending, from either above or below (see results for zone B in Wootton et al., 2000). The membrane clearly contributes to the overall rigidity of the structure by acting as a stressed skin and, for this to function in the shallow pleats of the remigium, the material needs to be stiff in tension. The

combination of a high Young's modulus with comparative thickness supplies this stiffness. There is some evidence that the modulus may increase somewhat along the span (Fig. 5) and that the membrane is appreciably thinner towards the wing tip (Fig. 7). The two would tend to cancel out.

The vannus operates very differently. Ablation shows that, here too, the membrane stiffens the deeply pleated structure to bending (Wootton et al., 2000), but both thickness and Young's modulus values are appreciably lower than in the remigium, so that the membrane is far less stiff. Examination of the hind wing of a flying tethered locust, illuminated stroboscopically to slow or stop the apparent stroke, shows that deep diagonal tension creases develop in the membrane of all the cells of the vannus as it develops camber by the umbrella effect during the downstroke. The cells clearly undergo appreciable shearing as a necessary part of the wing's deformation, and this is facilitated by the curved, flexible cross-veins, and the relatively thin, low-modulus membrane. A stiff membrane here would be disadvantageous, absorbing unnecessary muscular energy and causing undesirable stresses.

The lowest modulus values, below 1.5 GPa, were found at the perimeter of the vannus. Stress/strain curves here had a pronounced 'toe' region, indicating some initial strain before the membrane takes the full load. Scanning electron micrographs of the margin show a crimped band of cuticle just inboard of the edge (see Fig. 4G in Wootton et al., 2000). This is presumably an anti-tear device. Tension at the edge would extend this band, and the narrow outermost strip would tend to curl underneath, so that the maximum stress would be removed from the extreme margin. Tearing would otherwise tend to be checked by the network of cross-veins in the outer area of the fan.

The results from the polarising microscopy are no less interesting. The only region of the wing to show clear membrane birefringence is the leading-edge spar. This consists of the costal and subcostal veins and the radius, linked by abundant straight cross-veins, together forming a three-dimensional girder with a V-shaped cross-section (Wootton et al., 2000). Isolating the membrane destroys the birefringence, indicating that it is due to strain rather than to molecular orientation. Analysis, both by routine microscopy with a quarter-wavelength plate and using the automated microscope of Glazer et al. (1996), shows the pattern of strain within the cells to be complex, and more work is needed for a functional interpretation, but it is possible that pre-stress may help account for the results of bending tests on the leading-edge spar described by Wootton et al. (2000). In the specimens tested, the spar (zone A) was more rigid to bending from the dorsal side than from the ventral side. Furthermore, ablation of the membrane reduced the spar's rigidity when loaded from above, but had no effect on bending from below. This would be precisely the effect if the membrane were pre-stressed to resist bending from above. A force from below would then tend to eliminate the membrane stress, rendering it structurally neutral.

In conclusion, the membrane of the desert locust hind wing appears to be a versatile material whose properties vary appreciably from place to place in the wing, in accordance with local requirements. In the leading-edge spar, the membrane may be pre-stressed so as to minimise stress under the major loading of the downstroke. In the remainder of the remigium, it is stiff and relatively thick in association with its role, as a stressed skin, in supporting the shallow framework of veins (Wootton et al., 2000). This role to some extent continues in the vannus, but here the relative thinness and lower modulus values combine to allow more in-plane extension and out-of-plane creasing in association with the necessary deformation of the vannal cells in the automatic generation of camber during the downstroke. This creasing may be further assisted by membrane pre-crimping, particularly in the inner region of the vannus. Finally, along the vannus edge, tearing appears to be resisted by a crimped sub-marginal band.

This variation in properties occurs despite the apparent absence from the membrane of chitin, which is a major factor in determining the local properties of cuticle elsewhere. Why is it lacking in the wing membrane? In a species in which flight economy is paramount, the minimisation of wing mass may be extremely important, and the insects may have evolved to use the thinnest, lightest membrane whose properties are acceptable. The two mechanically functional layers of the epicuticle are always the first part of the cuticle to be secreted by the epidermis and may well be indispensable. Their thickness varies rather little, whereas that of the chitin-containing procuticle is highly variable. The logical final step in procuticle thinning is complete loss, and it appears that, in locusts at least, the epicuticle alone can provide all the strength and variability in stiffness necessary in the functioning of the wing. The chemical foundation for the variability is unclear, but presumably lies in local differences in the proteins concerned or in the degree of cross-linking or both.

This research was carried out with the assistance of BBSRC grants SO4798 and SO7722, BBSRC Special Studentship 3178, and the NERC Organic Mass Spectrometry Facility, School of Chemistry, Bristol University. We are grateful also to Professor A. M. Glazer and Dr J. G. Lewis of the Department of Physics, Oxford University, for the use of their automated optical imaging system.

## References

**Alexander, R. McN.** (1966). Rubber-like properties of the inner hinge-ligament of Pectinidae. *J. Exp. Biol.* **44**, 119–130.

**Andersen, S. O., Højrup, P. and Roepstorff, P.** (1995). Insect cuticular proteins. *Insect Biochem. Mol. Biol.* **25**, 152–176.

**Andersen, S. O., Peter, M. G. and Roepstorff, P.** (1996). Cuticular sclerotization in insects. *Comp. Biochem. Physiol.* **113**B, 698–705.

**Banerjee, S.** (1988a). Organisation of wing cuticle in *Locusta migratoria* Linaeus, *Tropidacris cristata* Linnaeus and *Romalea microptera* Beauvais (Orthoptera: Acrididae). *Int. J. Insect Morph. Embryol.* **17**, 313–326.

**Banerjee, S.** (1988b). The functional significance of wing architecture in acridid Orthoptera. *J. Zool., Lond.* **215**, 249–267.

**Credland, P. F.** (1978). An ultrastructural study of the larval

integument of the midge, *Chironomus riparius* Meigen (Diptera: Chironomidae). *Cell Tissue Res.* **186**, 327–335.

**Filshie, B. K.** (1982). Fine structure of the cuticle of insects and other arthropods. In *Insects Ultrastructure*, vol. 1 (ed. R. C. King and H. Akai), pp. 281–312. New York: Plenum Press.

**Glazer, A. M., Lewis, J. G. and Kaminsky, W.** (1996). An automated optical imaging system for birefringent media. *Proc. R. Soc. Lond. A* **452**, 2751–2765.

**Gosline, J. M.** (1980). The elastic properties of rubber-like proteins and highly extensible tissues. In *The Mechanical Properties of Biological Materials* (ed. J. F. V. Vincent and J. D. Currey), pp. 331–358. Cambridge: Cambridge University Press.

**Hepburn, H. R. and Chandler, H. D.** (1976). Material properties of arthropod cuticles: the arthrodial membranes. *J. Comp. Physiol*. **109**, 177–198.

**Jensen, M. and Weis-Fogh, T.** (1962). Biology and physics of locust flight. V. Strength and elasticity of locust cuticle. *Phil. Trans. R. Soc. Lond. B* **245**, 137–169.

**Ker, R. F.** (1977). Some structural and mechanical properties of locust and beetle cuticle. DPhil thesis, University of Oxford, UK.

**Lemburg, C.** (1998). Electron microscopical localization of chitin in the cuticle of *Halicryptus spinulosus* and *Priapulus caudatus* (*Priapulida*) using gold-labelled wheat germ agglutinin: phylogenetic implications for the evolution of the cuticle within the Nemathelminthes. *Zoomorph.* **118**, 137–158.

**Neville, A. C.** (1975). *Biology of the Arthropod Cuticle*. Berlin, Heidelberg: Springer.

**Neville, A. C.** (1980). Optical methods in cuticle research. In *Cuticle Techniques in Arthropods* (ed. T. A. Miller), pp. 45–89. Berlin: Springer-Verlag.

**Neville, A. C.** (1993). *Biology of Fibrous Composites: Development Beyond the Cell Membrane*. Cambridge: Cambridge University Press.

**Reynolds, S. E.** (1975). The mechanical properties of the abdominal cuticle in *Rhodnius*. *J. Exp. Biol.* **62**, 69–80.

**Richards, G. A.** (1951). *The Integument of Arthropods*. Oxford: Oxford University Press.

**Snodgrass, R. E.** (1935). *Principles of Insect Morphology*. New York, London: McGraw-Hill.

**Stankiewicz, B. A., van Bergen, P. F., Duncan, I. J., Carter, J. F., Briggs, D. E. G. and Evershed, R. P.** (1996). Recognition of chitin and proteins in invertebrate cuticles using analytical pyrolysis/gas chromatography and pyrolysis/gas chromatography mass spectrometry. *Rapid Com. Mass Spec*. **10**, 1747–1757.

**Vincent, J. F. V.** (1975). Locust oviposition: stress softening of the extensible intersegmental membranes. *Proc. R. Soc. Lond. B* **188**, 189–201.

**Vincent, J. F. V.** (1980). Insect cuticle: a paradigm for natural composites. In *The Mechanical Properties of Biological Materials* (ed. J. F. V. Vincent and J. D. Currey). *Soc. Exp. Biol. Symp*. **XXXIV**, 183–210.

**Vincent, J. F. V.** (1990). *Structural Biomaterials*, 2nd edition. Princeton: Princeton University Press.

**Vincent, J. F. V. and Hillerton, J. E.** (1979). The tanning of insect cuticle – a critical review and a revised mechanism. *J. Insect Physiol*. **25**, 653–658.

**Wainwright, S. A., Biggs, W. D., Currey, J. D. and Gosline, J. M.** (1976). *Mechanical Design in Organisms*. Princeton: Princeton University Press.

**Wasserthal, L. T.** (1996). Interaction of circulation and tracheal ventilation in holometabolous insects. *Adv. Insect Physiol.* **26**, 297–351.

**Weis-Fogh, T.** (1961). Molecular interpretation of the elasticity of resilin, a rubber-like protein. *J. Mol. Biol.* **3**, 648–667.

**Wootton, R. J.** (1995). Geometry and mechanics of insect hindwing fans–a modelling approach. *Proc. R. Soc Lond. B.* **262**, 181–187.

**Wootton, R. J.** (1999). Invertebrate paraxial locomotory appendages: design, deformation and control. *J. Exp. Biol.* **202**, 3333–3345.

**Wootton, R. J., Evans, K. E., Herbert, R. and Smith, C. W.** (2000). The hind wing of the desert locust (*Schistocerca gregaria* Forskål). I. Functional morphology and mode of operation. *J. Exp. Biol.* **203**, 2921–2931.